between the two configurations being likely very small. Support of this point of view is provided by the simultaneous presence in **6** of two coordination polyhedra showing symmetrical and unsymmetrical arrangement of the sulfur ligands.

On the basis of the preceding structural analysis, a structure where the copper atom is tetrahedrally coordinated by two tricyclohexylphosphine groups and by the sulfur atoms of the $PhHNCS_2^-$ ligand can be positively assigned to **11**.

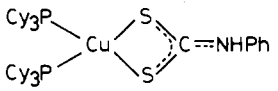

11

Dithiocarbamate complexes are obtained also when phenyl isothiocyanate is reacted with the η^1-BH_4 complexes **3** and **4**. Though the spectroscopic data concerning the *N*-phenyldithiocarbamate group are similar to those found for the η^2-S_2CNHPh complexes **10** and **11**, we believe that the dithiocarbamate ligand is unidentate in (triphos)Cu(S_2CNHPh) (**12**) and (np_3)Cu(S_2CNHPh) (**13**). This assumption is based on the structures of the corresponding formate, thioformate, and dithioformate complexes formed by (triphos)Cu and (np_3)Cu fragments.[1]

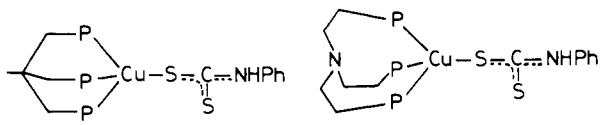

12 13

The formation of *N*-phenyldithiocarbamate complexes by reaction of the present copper(I) tetrahydroborates (eq 5) with

$$LCu(Bh_4) + 2SCNPh \rightarrow LCu(S_2CNHPh) + CNPh \quad (5)$$

$$[(PMe_3)_3PdH]BPh_4 + 2SCNMe \rightarrow [(PMe_3)_2Pd(S_2CNHMe)]BPh_4 + CNMe \quad (6)$$

SCNPh closely parallels that of the *N*-methyldithiocarbamate complex $[(PMe_3)_2Pd(S_2CNHMe)]BPh_4$ reported by Werner (eq 6).[31] Both of the above reactions represent unusual reactivity patterns of organo isothiocyanates, which usually insert into M–H bonds to give thioformamides.[32]

Conclusions

The number of metal tetrahydroborates that could find useful applications in the selective reduction of organic functional groups[33] is now increased by five units, namely $(PCy_3)_2Cu(BH_4)$, (triphos)$Cu(BH_4)$, $(PMePh_2)_3Cu(BH_4)$,[1] $(np_3)Cu(BH_4)$, and (etp_3)-$Cu(BH_4)$.[1] These complexes supply only a single hydride ion during the reduction, and their reducing capability seems to be influenced by the bonding mode of the BH_4^- ligand.[1]

The use of copper(I) tetrahydroborates in organometallic chemistry seems to be very promising as attested by the reactions reported in this present paper and in the preceding one. The diminished reducing capability of the coordinated BH_4^- group compared to that of the free ligand and the presence of (phosphine)copper fragments in the reaction mixture could lead in fact to the formation and stabilization of unusual chemical species.

The ease of making, handling, storing, and using (phosphine)copper(I) tetrahydroborate complexes represents a favorable feature of these reagents; conversely, their high molecular weight constitutes an unavoidable disadvantage.

Finally, we note the close analogies existing in the chemistry of metal hydrides and copper(I) tetrahydroborates, at least in their reactivity toward heteroallene molecules. Such analogies, which are reported in Scheme IV, lead to the conclusion that copper(I) tetrahydroborates could apparently function as substitutes for copper hydrides, very rare compounds, indeed limited to a few polynuclear species.[34]

Acknowledgment. This work was supported by a grant from the CNR program Chimica Fine e Secondaria. Thanks are due to F. Cecconi and G. Scapacci for technical assistance.

Registry No. **1**, 16903-61-0; **2**, 88637-65-4; **3**, 82678-89-5; **4**, 94500-07-9; **5**, 88927-05-3; **6**, 88279-91-8; **7**, 25263-83-6; **8**, 86322-44-3; **9**, 94517-75-6; **10**, 94517-76-7; **11**, 88622-22-4; **12**, 94500-08-0; **13**, 94500-09-1; $(PPh_3)_3Cu(ClO_4)$, 34010-81-6; CS_2, 75-15-0; SCNPh, 103-72-0; $HS_2CSCH_2SCS_2H$, 94500-10-4.

Supplementary Material Available: Listings of thermal parameters and structure factor amplitudes for $(PPh_3)_2Cu(\mu$-$S_2CSCH_2SCS_2)Cu(PPh_3)_2$, $(PPh_3)_2Cu(S_2COEt)$, and $(PPh_3)_2Cu(S_2CNHPh)$-$CHCl_3$ (68 pages). Ordering information is given on any current masthead page.

(31) Werner, H.; Bertleff, W. *Chem. Ber.* **1982**, *115*, 1012.
(32) Robinson, S. D.; Sahajpal, A. *Inorg. Chem.* **1977**, *16*, 2722.
(33) Sorrell, T. N.; Spillane, R. J. *Tetrahedron Lett.* **1978**, 2473; Fleet, G. W. J.; Fuller, C. J.; Hording, P. J. C. *Tetrahedron Lett.* **1978**, 1437. Kano, S.; Shibuya, S.; Ebata, T. *J. Heterocycl. Chem.* **1981**, *18*, 1239. Kametani, T.; Huang, S. P.; Nakayama, A.; Houda, T. *J. Org. Chem.* **1982**, *47*, 2328.
(34) Churchill, M. R.; Bezman, S. A.; Osborn, J. A.; Wormald, J. *Inorg. Chem.* **1972**, *11*, 1818. Lobkovskii, E. B.; Aripovskii, A. V.; Bel'skii, V. K.; Bulychev, B. M. *Sov. J. Coord. Chem. (Engl. Transl.)* **1982**, *8*, 49.
(35) Roberts, D. R.; Geoffrey, G. L.; Bradley, M. G. *J. Organomet. Chem.* **1980**, *198*, C75.
(36) Ashworth, T. V.; Nolte, M.; Singleton, E. *J. Organomet. Chem.* **1976**, *121*, C57.
(37) Albano, V. G.; Bellon, P. L.; Ciani, G. *J. Organomet. Chem.* **1971**, *31*, 75.

Contribution from the Research School of Chemistry, Australian National University, Canberra 2600, Australia, and Institut für Anorganische Chemie, Universität Bern, CH-3000 Bern 9, Switzerland

The Creutz–Taube Complex Revisited: Polarized Optical Spectroscopy

ELMARS KRAUSZ*† and ANDREAS LUDI‡

Received May 9, 1984

Attention is focused on the absorption and LD and MCD spectroscopy of the mixed-valence Creutz–Taube complex ion. The material is studied in a range of environments including solid solutions in PVA foils, microdispersed crystals in pressed KCl disks, and pure crystalline salts. These studies reveal a structure not shown in existing solution spectra as well as providing polarization information. Of particular interest is the strong polarization of the well-known "intervalence" transition near 6400 cm^{-1} as well as a broad and weaker absorption around 4000 cm^{-1} showing a large negative MCD. Evidence for vibronic coupling is presented.

Introduction

The strong polarization of the absorption region near 6400 cm^{-1} in the decaammine(μ-pyrazine-*N*,*N'*)diruthenium(5+) (C–T) mixed-valence ion was established only recently.[1] In this paper we fully describe these measurements as well as present further absorption experiments and magnetic circular dichroism (MCD)

†Australian National University.
‡Universität Bern.

(1) Fuerholz, U.; Buergi, H. B.; Wagner, F. E.; Stebler, A.; Ammeter, J. H.; Krausz, E.; Clark, R. J. H.; Stead, M.; Ludi, A. *J. Am. Chem. Soc.* **1984**, *106*, 121.

0020-1669/85/1324-0939$01.50/0

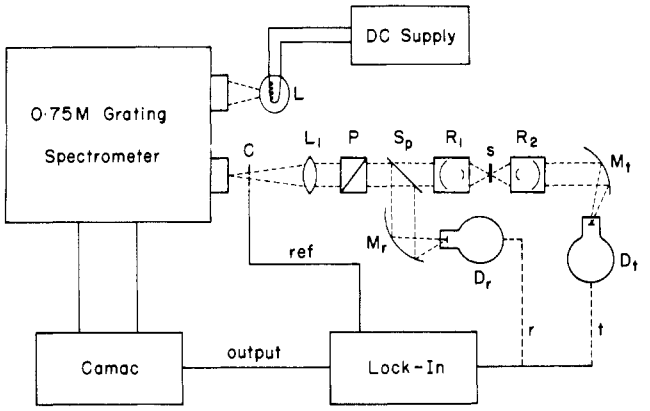

Figure 1. Microcrystal transmission and specular reflectance apparatus. Key: L, 200-W quartz halogen lamp powered by a stabilized dc power supply; C, 800-Hz tuning fork chopper; L_1, fused quartz lens; P, calcite Glan Taylor polarizer; S_p, 50% beam splitter; R_1 and R_2, 10× Beck reflecting objectives focusing light on sample S; $D_{r,(t)}$, InAs or InSb liquid-nitrogen-cooled detector; $M_{r,(t)}$ 5:1 off-axis ellipsoidal mirror. The subscripts r and t refer to positions of the detector for reflectance and transmission measurements, respectively. (See text.)

data in the region from 40 000 to 4000 cm^{-1}.

Much discussion and speculation[2] has developed as to the nature of the asymmetric band near 6400 cm^{-1}, and our experimental results allow a critical evaluation of current ideas as well as providing a basis for a more realistic theoretical model.

Materials

Chloride salts of the Creutz–Taube (C–T) ion and the oxidized [III,III] form and the tetrachlorozincate of its reduced [II,II] form were prepared as previously described.[1] Single crystals were grown by slow evaporation from aqueous solution.

Poly(vinyl alcohol) (PVA) foils were made by drying aqueous solutions containing dissolved plastic and the material on a glass surface. The pliable foils could then be easily removed upon evaporation of the solvent and were optically isotropic down to 2 K. Negligible depolarization of light occurred provided that crystallization did not occur during the drying process. Foils were quite stable though photochemical reduction did occur over a period of months.

Alternatively, salts were ground and pressed as KCl disks as is common practice for infrared (IR) spectra. When the powder was prepared in a dry glovebag, clear or transluscent disks with negligible or tolerable depolarization properties could be produced. These disks could be used for absorption and MCD measurements through the visible (vis) and ultraviolet (UV) regions, but factors such as particle size distribution and microcrystal reflectivities leave some doubt as to the quantitative aspects of materials dispersed in KCl even when apparently quite clear. Plastic foils provide a more reliably isotropic and homogeneous environment for MCD measurements.

Experimental Section

Microreflectance Spectroscopy. Polarized reflectance spectra at near-normal incidence on crystals smaller than 1 mm × 1 mm were obtained by using a reflecting objective and a liquid-nitrogen-cooled InAs or InSb detector based system (Figure 1).

Radiation from a 200-W quartz halogen lamp was dispersed by a 1704 SPEX monochromator fitted with a 1.6-μm blaze grating. Monochromatic light was then chopped at 800 Hz by a small tuning fork chopper mounted at the exit slit. A quartz collimating lens passed light through a calcite polarizer. Linearly polarized light then passed through a 50% beam splitter and then was focused on the sample by a 10× reflecting objective.[4] Specularly reflected light was then collected by the same optical element and 50% passed to the detector via a 5:1 off-axis ellipsoidal mirror. The output of the detector then went to a lock-in amplifier (PAR 124) whose output was digitized by a CAMAC based data logger that also controlled the scanning of the spectrometer.

This apparatus is a simple extension of the original work of Ferguson[4] who used reflecting objectives and the optics of a Cary 17 spectrophotometer to perform reflectance measurements in the visible region using a photomultipler detector. Our measurements in the UV–vis were made with the grating spectrometer again using a photomultipler replacing the cooled IR detector.

Data in digital form were then transferred to a PDP 11/45 for further processing and display. The system was calibrated by replacing the sample with a freshly evaporated aluminum surface that provided a 100% reflectivity level. Percent reflectance spectra were then obtained by division of the digitized data, and a reproducibility of better than 2% could be obtained for crystals of size 2 mm × 1 mm. Precision was limited by the quality of the crystal surfaces, the difficulty being that the crystals were both extremely soft and very water soluble.

Calibrated reflectance spectra taken in the range 0.8–2.5 μm were then Kramers–Kronig transformed by using the inverse Fourier technique of Sceats and Morris[3] to obtain absorbance spectra via the imaginary part of the refractive index.

Absorption Spectra. The same apparatus as described above was easily modified to measure transmission spectra.[4] A second reflecting objective placed behind the first collected transmitted light that was relayed to the detector. Spacing between the objectives is 3 cm, and this was adequate to allow a helium flow tube[4] containing the sample to pass between the objectives. Besides the simplicity of this system optically, data accumulated in this way have the advantage that small offsets can be corrected dynamically and as no separate reference beam is used, errors due to flow tube absorptions or optical imperfections are accurately balanced when an absorption spectrum is generated on the computer. This is done by simply calculating the log ratio of the transmission spectrum of the sample and that of a hole the same size as used to mount the sample.

This system easily allows measurement of crystals of 50-μm diameter or less with good resolution and excellent signal to noise ratio. Some spectra were also measured on a Cary 17 spectrophotometer fitted with reflective objectives in the sample beam,[4] again using the flow tube technique to obtain variable temperatures down to 5K.

MCD Spectra. Spectra in the range 1–2.5 μm were measured by a system based on the chopper, monochromator, and detector described above. The cooled detector was operated in photovoltaic mode with an Analog 50 J operational amplifier. A 57-kHz Infrasil photoelastic modulator was used to generate circularly polarized light. The three-lock-in technique of Naife et al.[5] was used to eliminate spurious signals due to acoustic pickup and minimize drift problems. A BOC 5-T superconducting solenoid provided the magnetic field, and the sample was placed in helium exchange gas or liquid helium. This is most important for work with PVA foils due to their very poor thermal conductance.

The two output lock-in amplifiers provide signals proportional to the total amount of transmitted radiation (TL) and the differential circular polarization (CP) of the radiation. The ratio of these quantities CP/TL is then proportional to $\Delta A = A_L - A_R$ (the circular dichroism) when the ratio is less than about 0.1. Previous workers[5,6] have generated this ratio electronically with a ratiometer or have used a servo system on the slit or lamp intensity (or a combination of both) to keep the detected value of TL constant. Both these approaches have problems with artifacts and dynamic range limitations. We have developed a technique capitalizing again on the power of digital processing techniques. Both TL and CP signals were simultaneously accumulated on a MINC/11 processor. The processor also controlled the spectrometer stepping motor and superconducting magnet power supply. MCD spectra were then accurately generated, paying careful attention to the zero offsets that plague ratiometer operation. The situation where $\Delta A > 0.1$ was also easily dealt with by calculating the correct logarithmic function. Accurate absorption spectra were generated in a manner analogous to that described for microcrystal absorbances.

Results

Reflectance Spectra. The polarized reflectance spectrum of the chloride salt is shown in Figure 2 along with the associated transformed absorption profile. When light is polarized parallel to the *c* axis of the crystal, very little dispersion of the reflectance is observed. With light polarized perpendicular to this axis there is a strong dispersion. From the known crystal structure[1] the *c*

(2) See, for example: Brown, D. B., Ed. "Mixed Valence Chemistry"; D. Reidel Publishing Co.: Dordrecht, 1980. Wong, K. Y.; Schatz, P. N. *Prog. Inorg. Chem.* **1981**, *28*, 370.
(3) Sceats, M. G.; Morris, G. C. *Phys. Status Solidi A* **1972**, *14*, 643.
(4) Ferguson, J. In "Electronic States of Inorganic Compounds: New Experimental Techniques"; Day, P. Ed.; D. Reidel Publishing Co.: Dordrecht, 1974; p 59. Day, P.; Ferguson, J. *J. Chem. Soc., Fardaday Trans 2* **1981**, *77*, 1588.
(5) Naife, L. A.; Keiderling, T. A.; Stephens, P. J. *J. Am. Chem. Soc.* **1976**, *98*, 2715.
(6) Osborne, G. A.; Cheng, J. C.; Stephens, P. J. *Rev. Sci. Instrum.* **1973**, *44*, 10. Mason, S. F. *Adv. Infrared Raman Spectrosc.* **1981**, 283.
(7) Schatz, P. N.; Piepho, S. B. "Group Theory and Spectroscopy"; Wiley Interscience: New York, 1983.
(8) Hush, N. S. in "Mixed Valence Chemistry"; Brown, D. B., Ed.; D. Reidel Publishing Co.: Dordrecht, 1980.

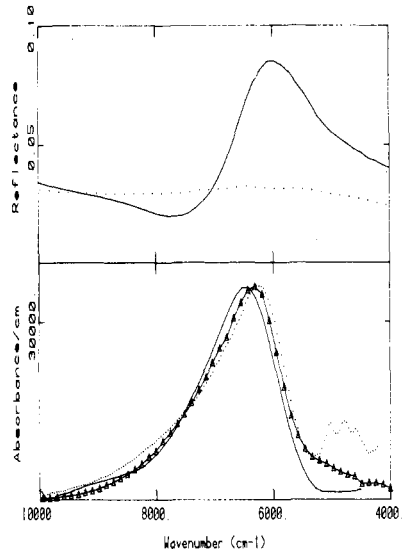

Figure 2. Upper panel: reflectance spectra Parallel (···) and perpendicular (—) to the c axis of a $[II,III]Cl_5$ single crystal at 300 K. Lower panel: transformed absorbance spectrum perpendicular to c (—); 300 K absorption spectra of a single crystal 30 μm thick of "doped" $[III,III]Cl_6$ (···); a PVA foil containing $[II,III](tos)_5$ with features due to the PVA material subtracted (-Δ-). Absorbances have been normalized to the transformed spectrum for comparison.

axis is parallel to the X axis of the chromophore. X is perpendicular to the interion (Z) direction and the plane of the pyrazine ring. This result clearly establishes the dominant polarization of the 6400-cm^{-1} band as being in the YZ plane, but, due to the occurrence of two dimers in the crystallographic ab plane, it is not possible to determine the ratio of Y to Z intensity.

Reflectance measurements made in the vis-UV region indicate that the strong visible absorption at 18 000 cm^{-1} has a similar polarization. A quantitative study in this region was not possible as the surface quality of the crystals was too variable for studies in the shorter wavelength region.

The absorbance spectrum transformed from this data compares reasonably well with that obtained from solution, KCl disk, single-crystal, and foil spectra as shown. Comparison, especially in the lower frequency regions, is limited by the cutoff of our reflectance measurements due to system optics at 4000 cm^{-1}. The reflectance in the ab polarization is not yet flat at the lowest available energy. The molar concentration of the crystal is 2.4 M, and when allowance is made for the orientation of the chromophores, the peak molar extinction of the ion in the crystal is 9500 M^{-1} cm^{-1} compared to the solution value of 5500 M^{-1} cm^{-1}.[9] Part of this discrepancy may arise from corrections due to the refractive index difference between the crystal and solution environments. It was not possible to obtain crystals thin enough to measure absorption spectra of the intense transition directly. Transmission spectra would have to be corrected for reflectance losses as well, but crystals of the oxidized $[III,III]Cl_6$ invariably undergo some photochemical reduction and contain a small (and convenient) amount of the mixed-valence species.

Absorption spectra measured in this way provide evidence that the peculiar asymmetry observed in the 6400-cm^{-1} transition is not greatly affected by any solvent or environmental effects.

Absorbance Spectra. Although it was not possible to measure the intense polarization directly in absorbance, except as the "doped" material in the $[III,III]Cl_6$ salt, it was found that reasonable transmission could be obtained from $[II,III]CL_5$ crystals when light was polarized parallel to the c axis of the crystal as long as it was not thicker than about 50 μm.

Figure 3 shows absorbance spectra of a $[II,III]Cl_5$ crystal at 300 and 10 K. These indicate a spectrum quite different from that seen in the YZ polarization spectra obtained from the

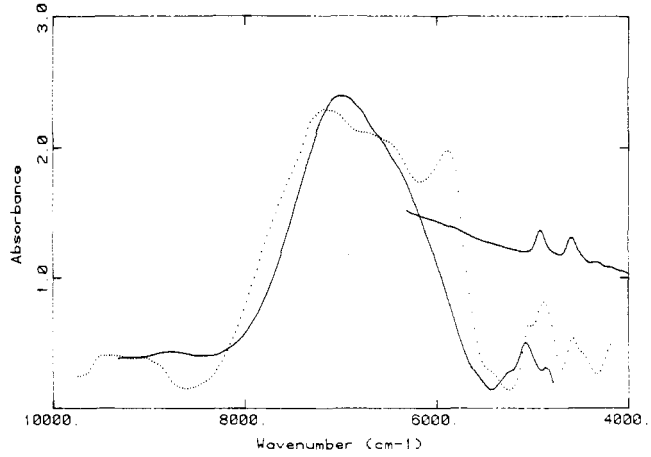

Figure 3. X-Polarized spectra of a 50-μm-thick crystal of $[II,III]Cl_5$ at 300 K (—) and 10 K (···). Inset is part of the absorption spectrum of a similar crystal of $[II,II](ZnCl_4)_2$ at 10 K showing common vibrational overtone features.

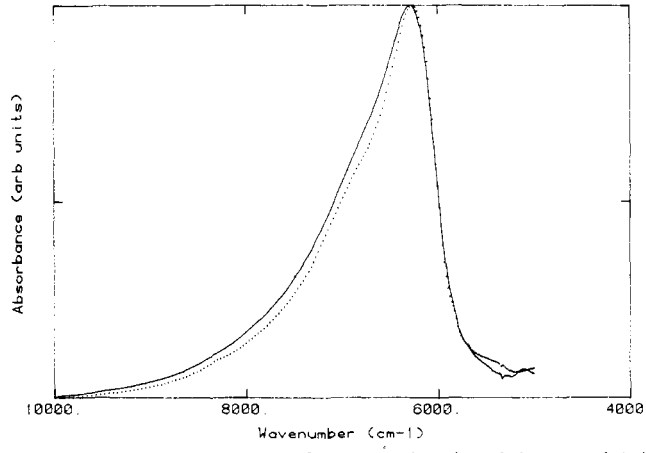

Figure 4. Absorption spectra of protonated (—) and deuterated (···) $[II,III](tos)_5$ in PVA at 10 K. Features due to the foils appearing below 5500 cm^{-1} have *not* been subtracted.

transformed reflectance and "doped" $[III,III]Cl_6$ spectra. Sharp low-energy features are common to $[II,II](ZnCl_4)_2$, $[II,III]Cl_5$, and $[III,III]Cl_6$ spectra and are easily assigned as combinations of NH and NH_3 vibrations. No other absorption is seen in the $[II,III]Cl_5$ spectra and only the "doped" 6400-cm^{-1} absorption in that of the $[III,III]Cl_6$.

The crystal structure of $[II,III]Cl_5$ determines that the spectra in Figure 3 are purely X polarized. The X-polarized absorptions are estimated to have an absorption intensity of the order of 1% of the dominant YZ-polarized transitions. They show considerable structure at low temperature and are generally shifted to higher energy compared to the YZ polarization. The observed lack of dispersion in the X polarization reflectance confirms that the absorbances measured are not distorted by reflectance effects. There does not seem to be any easily recognizable vibrational pattern or progression in the spectrum, but it is important to note that there is little if any intensity in the region below 6000 cm^{-1}. Single-crystal absorbance spectra of the $[II,III](tosylate)_5$ also show substantial (XY) absorbance, with the Y intensity dominating,[1] but its crystal morphology and less symmetric crystal structure preclude any quantitative measurements at this stage.

The ammine protons of the complex may be readily exchanged in acid/D_2O solution. Figure 4 shows the effect of such deuteration on the main 6400-cm^{-1} system. Spectra are measured at 10 K in PVA and PVA dissolved in D_2O, which also exchanges the OH protons in the foil. Comparison of the normalized protonated and deuterated spectra reveals a vanishing spectral shift of the low-energy edge, but a substantial change in absorption profile at higher energies. The asymmetric shape is more clearly resolved into a definite shoulder in the deuterated foil. The change

(9) Creutz, C.; Taube, H. *J. Am. Chem. Soc.* **1969**, *91*, 3988; **1973**, *95*, 1086.

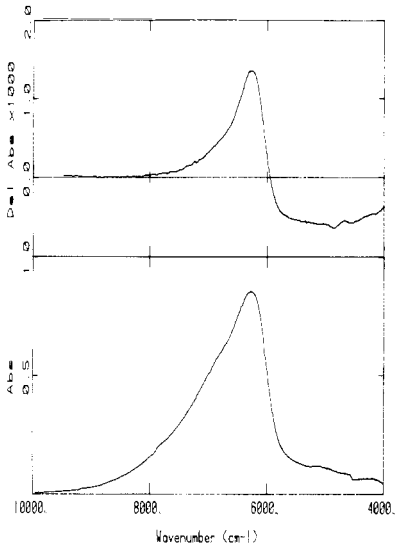

Figure 5. NIR absorption (lower panel) and MCD (upper panel) at 4.3 K and 4.5 T of a PVA foil of the dissolved $[II,III](tos)_5$ salt. Low-energy absorption features due to the foil have been subtracted, and the residual absorption in this region is due to the C–T ion itself.

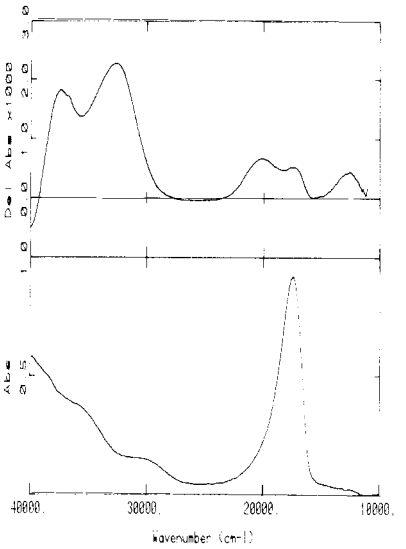

Figure 6. Vis–UV absorption (lower panel) and MCD (upper panel) at 4.3 K and 4.5 T of a dilute PVA foil of $[II,III](tos)_5$.

of the asymmetry upon deuteration has significant implications as to the assignment of the peculiar shape of the transition.

MCD Spectra. MCD requires an isotropic propagation direction within a material, and single-crystal measurements are precluded by conditions of crystal symmetry, absorption intensity, and crystal size. Most of our measurements have been made in PVA foils though general features are duplicated in KCl disks that can be considered to be solid solutions when the particle size becomes smaller than the wavelength of the radiation involved.

The MCD spectrum of a PVA foil in the near-infrared (near-IR) region shown in Figure 5 reveals that the MCD of the main band at 6400 cm^{-1} is relatively weak. All the features observed show a characteristic $1/T$ dependence of amplitude in the range from 2 to 50 K and are thus assigned as MCD C terms.[7] The value of the ratio of $\Delta A/A$ measured at 6250 cm^{-1}, extrapolated to the limit of $g\beta H/kT \ll 1$ (assuming only a C-term contribution to the dichroism) is estimated as <0.005. Existing models for the absorption intensity of the C–T ion would predict no MCD at all, as no absorption intensity in the X or Y polarizations is forcast. The MCD intensity itself however is consistent with an approximately 1% or greater (XY) polarization of the absorption intensity with Z-polarized intensity dominating. Measurements of the saturation behavior of the MCD at 4.17 and 1.87 K and fields up to 5 T at 6250 cm^{-1} show a characteristic curvature that can be fitted to a single Kramers doublet with a g of 2.17 ± 0.02. Although a full analysis of the saturation behavior requires a knowledge of the XY and Z dipole strengths, it is interesting to note that the effective g is reasonably close to the g_Z value of 2.45 obtained from singel-crystal EPR measurements.[1]

Notable in the MCD spectra is a large (relative to the absorption in this region) negative dichroism in the region <6000 cm^{-1}. This signal must arise from a weak absorption not detected in previous work. Figure 5 gives the absorption spectrum of a foil with features due to the PVA material itself subtracted. A region of broad absorption is clearly indicated. We note again that this absorption is not seen in the X polarization of the $[II,III]Cl_5$ single-crystal data but is apparent in foil and KCl disk spectra and spectra "doped" in the $[III,III]Cl_6$ as host where the polarization is not clearly defined. Deuteration of the PVA foil and ammine protons does not greatly change the MCD spectra of the strongly allowed band although there is some variation in shape of the region near 4000 cm^{-1}.

The shoulder responsible for the asymmetry of the 6400-cm^{-1} band is much less pronounced in the MCD spectrum. This as well as the different linear polarization properties of the absorption indicates either that there is more than one electronic state involved in the absorption profile or that nontotally symmetric (referred to the dimer) vibrations are involved. The suggestion made by Hush[8] that the high-energy shoulder was due to a totally symmetric mode is initially rejected by our MCD data.

The MCD in the UV–vis region is shown in Figure 6. Again, temperature-dependence studies show that all features are C terms to within experimental error. The MCD intensity in the UV–vis region is also quite weak (of comparable $\Delta A/A$ as that seen in the near IR), and its dispersion indicates that it does not originate predominantly from the intense absorption that gives the material its purple color. MCD C terms normally are expected to have the same shape as the absorption to the same (spin–orbit) level.[7] A low-energy absorption shoulder at 12900 cm^{-1}, reported in the original work of Creutz and Taube,[9] does give a (relatively) strong positive signal. There are two other features at 20400 and 17400 cm^{-1} that do not clearly align with the single strong band seen in absorption at 18200 cm^{-1}.

Discussion

The strong polarization of the 6400-cm^{-1} band is clearly established although a significant 1% of this intensity is seen in the X direction. This strong polarization ratio is not at all unexpected or unreasonable as the absorption intensity in a mixed-valence material arises basically from the transfer of charge from one metal center to the other (this is defined as the Z direction). More surprising is the level of intensity in the X direction. Also there must be considerable Y intensity to account for the substantial MCD in the <6000-cm^{-1} region. It has been shown that within the PKS vibronic coupling model[10] (which encompasses most other models) the introduction of spin–orbit coupling does not induce any intensity in the X or Y direction.

The measured MCD *must* involve transverse (to Z) intensity directly. Pure linear polarization does not give rise to magnetic optical activity.

The intense absorption seen in the visible region is usually assigned as a metal-to-ligand charge transfer from Ru^{2+} to the pyrazine ligand or, within a molecular orbital framework, as a $b_{3u} \leftarrow b_{2g}$ transition. As (paramagnetic) C terms dominate the MCD of this region also, it is not feasible to envisage the transfer originating from a localized Ru^{2+} as the latter is diamagnetic. This transition also must be considered in the overall electronic structure of the dimer. In zeroth order, the low-energy shoulder at 12800 cm^{-1} perhaps may be envisaged as a singlet–triplet charge transfer corresponding to the allowed singlet–singlet transition at 18200 cm^{-1}, but the separation involved does seem large as the spin–orbit coupling parameter for Ru^{3+} is usually given as ~1000 cm^{-1}. A

(10) Piepho, S. B.; Krausz, E. R.; Schatz, P. N. *J. Am. Chem. Soc.* **1978**, *100*, 2996.

large number of states arise from coupling the d^5 core to the pyrazine anion within the dimer. It seems more appropriate to concentrate on the low-energy transitions that are so unique to the C-T mixed-valence ion.

In the <6000-cm^{-1} energy region our MCD data have unveiled a broad (YZ-) polarized transition extending beyond the range of our current instrumentation. Structure and X intensity within the 6400-cm^{-1} system are also not envisaged by current models, and we are forced to consider both the contribution of electronic structure within the t_2^5 basis of the dimer system and vibronic activity (involvement of nontotally symmetric modes of vibration that change the overall symmetry of an electronic vibrational state).

Starting from a basis consisting of Ru^{2+} with its filled t_2^6 configuration and Ru^{3+} as basically a hole in this filled shell, it is clear that electronic splittings of the order of 1000 cm^{-1} must originate in the structure of the t_2^5 configuration. Vibrational energies are also in the range 200-2000 cm^{-1}. The e_g orbitals on the metal and the π^* orbitals on the ligand are clearly well separated in energy from the t_2 orbitals. The effects of spin-orbit coupling and low symmetry will split the t_2^5 configuration into three Kramers doublets. Upon introduction of an interaction between the two centers and formation of states consistent with the observed equivalence of the two ruthenium centers, six levels will ensue, three gerade and three ungerade. In the most general case, three electric dipole allowed transitions would be expected with energy separations of the order of the spin-orbit splitting on Ru^{3+} and the specific interion interaction energy. The inclusion of vibronic coupling could then be envisaged in a manner analogous to that used by Piepho, Krausz, and Schatz.[10] Such an analysis is in progress.[11]

(11) Schatz, P. N.; Neuenschwander, K., personal communication.

Our deuteration results indicate that the high-energy shoulder is most likely a vibrational sideband system of the stronger pure electronic region at lower energy that does not shift on deuteration. As noted the MCD result precludes this being a simple Franck-Condon coupling to a totally symmetric mode, and we conclude that vibronic activity is present but not dominant.

The mystery of the Creutz-Taube ion seemingly originates in a fine balance between the specific interaction between the two metal centers, the back-bonding character of Ru^{2+}, the weak forward bonding of Ru^{3+} toward the pyrazine ligand, and the spin-orbit and low-symmetry fields that may tend to reduce vibronic effects. A simple model concentrating on the electronic coupling has been formulated by Dubicki, Ferguson, and Krausz.[12] Comparison with experiment is somewhat limited by lack of data in the region below 4000 cm^{-1} where the third electronically allowed dimer feature is expected. These low-energy features are primarily due to the Ru^{3+} single ion. Measurements on other strongly interacting mixed-valence dimers are also necessary. We are working toward both these goals.

Acknowledgment. E.K. acknowledges the assistance of Dr. R. J. Robbins in programming the Kramers-Kronig transform of the reflectance data and helping at all phases of data processing. The help and encouragement of Dr. J. Ferguson at all phases of this work have been essential. Some initial MCD measurements were done in collaboration with Dr. H. U. Guedel and performed at the University of Virginia with support from Prof. P. N. Schatz. There have been many fruitful discussions with Dr. L. Dubicki and Dr. S. B. Piepho.

Registry No. [II,II]$(ZnCl_4)_2$, 87922-19-8; [II,III]Cl_5, 94780-98-0; [II,III]$(tos)_5$, 41557-38-4; [III,III]Cl_6, 94750-87-5.

(12) Dubicki, L.; Krausz, E. R.; Ferguson, J., submitted for publication in *J. Am. Chem. Soc.*

Contribution from the Institut für Anorganische Chemie and Laboratorium für Kristallographie, Universität Bern, CH-3000 Bern 9, Switzerland

The Creutz-Taube Complex Revisited: Crystallographic Study of the Electron-Transfer Series $[(NH_3)_5Ru(pyz)Ru(NH_3)_5]^{n+}$ (n = 4-6)

URS FÜRHOLZ,[1a] STEFAN JOSS,[1a] HANS BEAT BÜRGI,*[1b] and ANDREAS LUDI*[1a]

Received May 9, 1984

The crystal and molecular structures of the following four compounds have been determined: $[(NH_3)_5Ru(pyz)Ru(NH_3)_5](ZnCl_4)_2$ (pyz = pyrazine), [II,II], orthorhombic, *Pcab*, a = 11.348 (2) Å, b = 11.614 (2) Å, c = 22.144 (3) Å, Z = 4, R = 2.5% for 2178 reflections; $[(NH_3)_5Ru(pyz)Ru(NH_3)_5]Cl_5 \cdot 5H_2O$, [II,III], orthorhombic, *Pnnm*, a = 17.595 (2) Å, b = 11.308 (2) Å, c = 7.021 (1) Å, Z = 2, R = 2.4% for 1023 reflections; [II,III]$(tos)_5 \cdot 4H_2O$ (100 K, tos = *p*-toluenesulfonate), triclinic, $P\bar{1}$, a = 13.162 (3) Å, b = 15.116 (5) Å, c = 15.749 (5) Å, α = 106.96 (2)°, β = 94.40 (2)°, γ = 103.15 (2)°, Z = 2, R = 3.2% for 5304 reflections; $[(NH_3)_5Ru(pyz)Ru(NH_3)_5]Cl_6 \cdot 2H_2O$, [III,III], monoclinic, $P2_1/n$, a = 7.465 (2) Å, b = 11.401 (2) Å, c = 14.613 (2) Å, β = 79.60 (2)°, Z = 2, R = 2% for 2503 reflections. Important average distances are in the order [II,II], [II,III], [III,III]: Ru-N(pyz) = 2.013 (3), 1.991 (9), 2.15 (1) Å; Ru-NH_3(trans) = 2.149 (3), 2.123 (7), 2.089 (1) Å; Ru-NH_3(cis) = 2.132 (3), 2.112 (3), 2.101 (5) Å; C-N = 1.353 (4), 1.362 (4), 1.341 (2) Å; C-C = 1.363 (5), 1.361 (5), 1.382 (2) Å. The overall geometries of the binuclear ions in all four compounds are very similar and are adequately described by an eclipsed arrangement of the two mononuclear subunits, with the pyrazine plane bisecting the *cis*-Ru-NH_3 bonds. The geometry of the [II,III] ion cannot be explained as the average of the geometries of [II,II] and [III,III]. The crystallographic results are compatible with two equivalent ruthenium atoms in the mixed-valence ion and demonstrate the significance of the ruthenium-pyrazine, t_{2g}-π^* bonding.

Introduction

Current models[2] for mixed-valence compounds distinguish between two limiting situations: class II or localized vs. class III or delocalized. The first case corresponds to a two-minima energy surface, a classical example is Prussian Blue with only weak coupling between Fe(II) and Fe(III). The second case corresponds to a single-minimum potential. Intermediate cases are represented by double-minimum wells with a separating barrier on the order of or smaller than thermal energy. These models have been extended by Schatz and co-workers (PKS model[3]) by introducing vibronic and electronic coupling between the two Ru subunits. Their description extracts the relevant model parameters by fitting position, intensity, and shape of the intervalence band to the experimental data. Let us emphasize that these models do not take into account the electronic structure of the bridging ligand

(1) (a) Institut für Anorganische Chemie. (b) Laboratorium für Kristallographie.
(2) Robin, M. B.; Day, P. *Adv. Inorg. Chem. Radiochem.* **1967**, *10*, 247. Hush, N. S. *Prog. Inorg. Chem.* **1967**, *8*, 391.
(3) Wong, K. Y.; Schatz, P. N. *Prog. Inorg. Chem.* **1981**, *28*, 369.

0020-1669/85/1324-0943$01.50/0